Accepted Manuscript

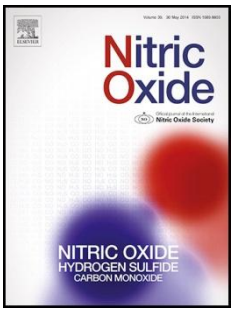

Title: Kinetic and thermodynamic studies on the disulfide-bond reducing potential of hydrogen sulfide

Author: Anita Vasas, Éva Dóka, István Fábián, Péter Nagy

PII: S1089-8603(14)00510-2
DOI: http://dx.doi.org/doi: 10.1016/j.niox.2014.12.003
Reference: YNIOX 1454

To appear in: *Nitric Oxide*

Received date: 30-8-2014
Revised date: 3-12-2014
Accepted date: 8-12-2014

Please cite this article as: Anita Vasas, Éva Dóka, István Fábián, Péter Nagy, Kinetic and thermodynamic studies on the disulfide-bond reducing potential of hydrogen sulfide, *Nitric Oxide* (2014), http://dx.doi.org/doi: 10.1016/j.niox.2014.12.003.

Kinetic and thermodynamic studies on the disulfide-bond reducing potential of hydrogen sulfide

Anita Vasas[1,2], Éva Dóka[1,2], István Fábián[2] and Péter Nagy[1*]

[1]*Department of Molecular Immunology and Toxicology, National Institute of Oncology, Ráth György utca 7-9, Budapest, Hungary, 1122*

[2]*Department of Inorganic and Analytical Chemistry, University of Debrecen, Egyetemtér 1, Debrecen, Hungary, 4010*

Running Head: Mechanisms of disulfide reduction by sulfide

***Address for Correspondence:**

Péter Nagy, PhD

Department of Molecular Immunology and Toxicology

National Institute of Oncology

1122 Budapest, Ráth György utca 7-9, Hungary

Email: peter.nagy@oncol.hu

Tel.: +36-1-224-8600/3644

Fax: +36-1-224-8620

Abstract

The significance of persulfide species in hydrogen sulfide biology is increasingly recognized. However, the molecular mechanisms of their formation remain largely elusive. The obvious pathway of the reduction of biologically abundant disulfide moieties by sulfide was challenged on both thermodynamic and kinetic grounds. Using DTNB (5,5'-dithiobis-(2-nitrobenzoic acid), also known as Ellman's reagent) as a model disulfide we conducted a comprehensive kinetic study for its reaction with sulfide. The bimolecular reaction is relatively fast with a second-order rate constant of 889 ± 12 $M^{-1}s^{-1}$ at pH = 7.4. pH dependence of the rate law revealed that the reaction proceeds via the bisulfide anion species with an initial nucleophilic thiol-disulfide exchange reaction to give 5-thio-2-nitrobenzoic acid (TNB) and TNB-persulfide with a pH independent second-order rate constant of 1090 ± 12 $M^{-1}s^{-1}$. However, kinetic studies and stoichiometric analyses in a wide range of reactant ratios together with kinetic simulations revealed that it is a multistep process that proceeds via kinetically driven, practically irreversible reactions along the disulfide → persulfide → inorganic polysulfides axis. The kinetic model postulated here, which is fully consistent with the experimental data, suggests that the TNB-persulfide is further reduced by sulfide with a second-order rate constant in the range of 5×10^3 – 5×10^4 $M^{-1}s^{-1}$ at pH 7.4 and eventually yields inorganic polysulfides and TNB. The reactions of cystine and GSSG with sulfide were found to be significantly slower and to occur via more complicated reaction schemes. ^{1}H NMR studies suggest that these reactions also generate Cys-persulfide and inorganic polysulfide species, but in contrast with DTNB, in consecutive equilibrium processes that are sensitive to changes in the reactant and product ratios. Collectively, our results demonstrate that the reaction of disulfides with sulfide is a highly system specific process from both thermodynamic and kinetic aspects, which together with the

considerable steady-state concentrations of the reactants in biological systems signifies physiological relevance.

Keywords
Hydrogen sulfide, disulfide reduction, persulfide, kinetics and mechanisms, speciation

Highlights

- Mechanistic study was conducted for the reduction of model disulfides by sulfide
- Kinetic properties and product speciation were found to be highly system specific
- The initial bimolecular reaction is a thiol-disulfide exchange via HS^-
- Persulfides are further reduced by sulfide in faster reactions compared to disulfides
- Multistep reactions proceed along the disulfide$\rightleftharpoons$persulfide$\rightleftharpoons$inorganic polysulfides axis

1. Introduction

The seminal discovery by Abe and Kimura, that endogenously produced hydrogen sulfide[1] acts as a neuromodulator [1], resulted in a paradigm shift and directed the focus of sulfide biology from toxicological studies [2] to essential biological functions in the last decade [3,4,5]. The blossom of this new field of research was demonstrated by the great number of excellent studies reporting a diverse array of sulfide-mediated biological processes at the 3rd international conference on sulfide biology [6].

The conference also highlighted that the ever increasing number of intriguing new discoveries and related controversies (that is a usual side effect of popular, rapidly developing research areas) now entails more and more mechanistic chemical studies in order to elucidate and reconcile the molecular mechanisms of sulfide's biological actions. One of the key areas of interest is the formation of persulfides on peptide and protein cysteine (Cys) residues and their potential role in sulfide signaling [7,8]. Persulfide species were proposed to be highly abundant in cellular systems with a plethora of likely biological functions that include i) serving as important intermediates in sulfide trafficking and/or buffering [9,10,11] ii) enhancing [12,13,14] or inhibiting [15,16,17,18] key enzymatic functions as well as iii) protecting against oxidative stress and mediating redox signaling events [7,9,19].

Importantly, from the chemical perspective, persulfides are oxidative posttranslational modifications of Cys residues [20]. Hence, their formation could occur either via the reaction of reduced Cys residues by oxidized sulfide species such as polysulfides [17] or via the reaction of oxidized Cys derivatives with reduced sulfide [10]. The reduction of biological disulfide species by sulfide was proposed to be a potential source of persulfides [21,22,23,24]. Notwithstanding, based on kinetic or thermodynamic considerations, the prevalence of this pathway in biological

systems is often questioned [25,26,27,28,29]. However, to our knowledge a comprehensive mechanistic study of the title reaction has thus far not been performed. Therefore, the aim of this contribution is to provide a deeper chemical insight into the kinetics, mechanisms and thermodynamic nature of disulfide reduction reactions by sulfide in order to assess the biological feasibility of these reactions. Our results highlight that persulfide formation via sulfide-mediated disulfide reduction is a highly system specific process both from the kinetic and thermodynamic points of view. We demonstrate that depending on the chemical properties of the corresponding disulfide moiety i) the rate of sulfide-mediated disulfide reduction varies on a large scale and ii) thermodynamically it represents a multistep equilibrium process, where the distribution of the oxidizing equivalent (coming from the disulfide) at physiological pH can lie anywhere along the disulfide $\rightleftharpoons$ persulfide $\rightleftharpoons$ inorganic polysulfides axis.

2. Materials and Methods

2.1. Reagents. All chemicals were analytical reagent grade or better and purchased from Sigma-Aldrich, St Louis unless indicated otherwise. The reagent solutions were prepared by using deionized and ultrafiltered water obtained from a Milli-Q system, Millipore (resistivity ≥ 18 MΩ cm), except for the NMR measurements, which were carried out in D_2O (99,9 % atom D). Buffer solutions were made using solid $Na_2HPO_4 \times 2H_2O$, KH_2PO_4, $Na_2B_4O_7 \times 10H_2O$ and NaOH for the kinetic or spectrophotometric studies or K_3PO_4 and D_2SO_4 (Alfa Aesar, 96 %, in D_2O, Karlsruhe, Germany) for the NMR experiments.

Sulfide stock solutions were prepared fresh daily in water using $Na_2S \times 9H_2O$ (ACS reagent, ≥ 98 %). $Na_2S \times 9H_2O$ crystals were stored under argon (4.0, Messer, Krefeld, Germany) and were thoroughly washed before dissolving them in ultrapure water. The basic stock solutions were kept on ice in the dark in sealed plastic centrifuge tubes to avoid oxidation and H_2S volatilization. The concentration of sulfide was determined by two different UV-VIS spectrophotometric methods as described previously [10]. Working solutions were prepared from stock solutions immediately before the measurements by dilution with the adequate buffer.

2.2. pH measurements. pH measurements were performed by a Metrohm 785 DMP Titrino with a double-junction combined pH glass electrode (Metrohm 6.255.100), calibrated using potassium hydrogen phthalate (pH 4.008) and sodium tetraborate (pH 9.177) standard solutions.

2.3. UV/VIS spectrophotometry. Electronic spectra were measured with a Perkin Elmer Lambda 2S UV/VIS double-beam spectrophotometer using quartz cells with calibrated 1 cm path lengths.

2.4. Spectral changes in the UV region upon the reaction of sulfide with DTNB. Equal volumes of freshly prepared sulfide and DTNB stock solutions were mixed under rigorous vortexing condition in 100 mM phosphate buffer at pH = 7.40 and I = 1 M (set with NaCl) to give the final concentrations of $[\text{sulfide}]_{tot}$ = 50 μM and [DTNB] = varied in the range of 5 – 25 μM. UV-spectra were recorded within 6 minutes after mixing.

2.5. Kinetic studies. Kinetic measurements were made with an Applied Photophysics DX-17 MV sequential stopped-flow apparatus using a 150 W Xe arc lamp. The reactions were followed by the decay of DTNB (at λ = 320 nm) and the formation of TNB (at λ = 412 nm). All kinetic traces were collected at 1 M ionic strength (defined by the buffer at the given pH and NaCl). The temperature was maintained at 25 °C in the observation cell with a Julabo F12 thermostat during the kinetic runs.

2.5.1. Sulfide and DTNB concentration dependencies. Kinetic runs were performed under pseudo-first-order conditions using a ≥ 10 fold excess of either sulfide or DTNB in 100 mM phosphate buffer at pH 7.40. Concentrations: *DTNB excess:* [DTNB] = 10 – 600 μM, $[\text{sulfide}]_{tot}$ = 0.25 – 60 μM; *sulfide excess:* [DTNB] = 1 – 30 μM, $[\text{sulfide}]_{tot}$ = 10 – 500. At least 3 kinetic runs were made and averaged at each concentration to establish the corresponding kinetic traces. The experiments were repeated in 14 and 11 sets of independent experiments for excess DTNB and excess sulfide using freshly prepared solutions, respectively. Error bars in the corresponding figures represent the standard deviations of independent experiments.

2.5.2. pH dependence. The pH was maintained by 100 mM phosphate (at 8.20 > pH > 6.20) or borate (at 9.97 > pH > 9.21) buffers and the ionic strength was adjusted to 1 M (NaCl).

Kinetic runs were performed under pseudo-first-order conditions using a ≥ 10 fold excess of sulfide or DTNB. When sulfide was used in excess, measurements were performed in 4 sets of independent experiments with DTNB concentrations in the range of 1 – 25 μM and sulfide concentrations in the range of 50 – 500 μM. At an excess of DTNB the data were collected in 9 sets of independent experiments with [DTNB] = 50 – 500 μM and [sulfide] = 1 – 5 μM.

2.5.3. Kinetics of L-cystine and oxidized glutathione (GSSG) with sulfide. Kinetic traces were collected under pseudo-first-order conditions using a ≥ 10 fold excess of sulfide (in the range of 15 - 35 mM) at constant 1.5 mM disulfide concentrations and pH = 7.4 in 100 mM phosphate buffer at 25°C and I = 1 M (NaCl). The kinetics at an excess of disulfide could not be investigated due to limitations in the solubility of the disulfide and small absorbance changes. Kinetic traces were collected at λ = 300 nm.

2.6. NMR experiments. ^{1}H-NMR spectra in the sulfide - L-cystine system were recorded by a Bruker AM 360 MHz (8.5 T) NMR spectrometer (Oxford, United Kingdom). The chemical shifts are reported in ppm, using DSS (4,4-dimethyl-4-silapentane-1-sulfonic acid) as an external standard with δ = 0.00 ppm. In order to reach chemical equilibria, reaction mixtures were incubated for 12 min before the spectra were recorded. Concentrations: [L-cystine] = 3.0 mM, $[sulfide]_{tot}$ = 0 - 40 mM at pD = 7.40 or 8.00 (pD = pH* + 0.4, where pH* is the uncorrected pH meter reading) in 225 mM deuterated phosphate buffer (made by dissolving K_3PO_4 in D_2O and setting the pD using D_2SO_4). Polysulfides in sulfide stock solutions were generated by mixing 101 mM OCl^- with 404 mM sulfide in deuterated phosphate buffer at pD = 8.00 [19]. The remaining sulfide concentrations were estimated based on the assumption that 1 mol HOCl

consumes 2 mols of sulfide to give 1 mol of polysulfide, which is a slight underestimate in light of the appropriate polysulfide distribution under the applied conditions (reaction 4).

2.7. Simulation and data analysis. Exponential fitting of the experimental kinetic traces were achieved by Micromath Scientist (2.01, Micromath Research, Saint Louis, Missouri, USA) or Applied Photophysics Pro-Data Viewer (4.2.0, Applied Photophysics Ltd, Leatherhead, Surrey, UK) softwares and the concentration and pH dependencies of the pseudo-first-order rate constants were fitted with Microsoft Excel 2010 and Micromath Scientist (2.01, Micromath Research, Saint Louis, Missouri, USA) softwares, respectively. NMR spectra were analyzed with MestReNova (8.1.2-11880, 2013, Mestrelab Research, Santiago de Compostela, Spain) software package.

Kinetic simulations were carried out with Micromath Scientist (2.01, Micromath Research, Saint Louis, Missouri, USA) software using the error controlled Runge-Kutta method. The model and parameter sets are described in detail in the Supporting Information document.

All data were illustrated using Microsoft Excel 2010.

3. Results

3.1. Products and stoichiometry of the reaction of DTNB with sulfide

In order to investigate the disulfide-bond reducing potential of sulfide we first used DTNB as a model compound. DTNB is a water soluble aromatic disulfide, which is often used in biochemistry as a reagent (Ellman's reagent) for quantitative measurement of total reduced thiol/sulfhydryl groups [30]. The assay is based on a thiol-disulfide exchange reaction [31], where a nucleophilic attack of the Cys thiol on the DTNB disulfide bond results in a mixed Cys-TNB disulfide and release 1 molar equivalent of the highly absorbing TNB (ε_{412} = 14100 $M^{-1}cm^{-1}$ [32] (reaction 1), which is quantified by spectrophotometry.

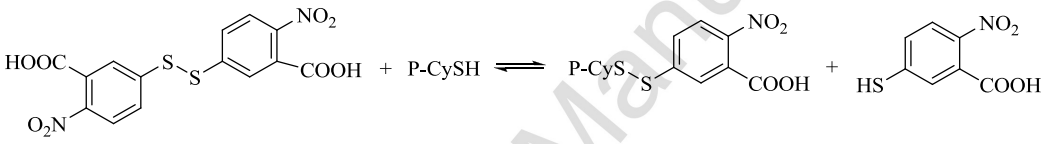

(1)

Sulfide, as the smallest thiol, also reduces DTNB to give the characteristic band of TNB at 412 nm (Figure 1).

Nashef, AS et. al. suggested that this reaction can be utilized for sulfide quantitation in aqueous media [33]. However, in contrast to Cys thiols they found that sulfide produced two molar equivalents of TNB at a slight excess of DTNB over sulfide. Furthermore, they reported that the oxidizing equivalents from the DTNB disulfide were transferred on to sulfide to eventually yield stoichiometric amounts of elemental sulfur, which was detected and quantified using an organic extraction protocol. However, we observed no sulfur precipitation upon the sulfide-mediated reduction of DTNB in our reaction mixtures and therefore propose that the sulfane sulfur containing products are most likely inorganic polysulfides.

In this study we revisited the stoichiometry of the reaction of sulfide with DTNB in a wider concentration range and at different DTNB : sulfide ratios. When sulfide was used in excess over DTNB, 2 TNB molecules were produced per DTNB (Table 1A).

A

In contrast, one sulfide liberated only one TNB at a high excess of DTNB (Table 1B). However, at < 100 fold excess of DTNB over sulfide, more than 1 sulfide equivalent of TNB production was observed and a decrease in the DTNB : sulfide ratio resulted a gradual increase in the amount of released TNB per sulfide molecule (Table 1B), suggesting that TNB is produced in a multistep process. In agreement with these observations we propose that in the first reaction step, a simple thiol-disulfide exchange reaction gives 1 mol equivalent of TNB and 1 TNB-persulfide species. TNB-persulfide is then reduced by sulfide to give another TNB and the polysulfide precursor HSSH. Subsequently, HSSH either reacts with another TNB-persulfide or disproportionates to eventually yield polysulfides, the composition and distribution of which depend on the applied conditions.

B

$$RSSR + H_2S \rightleftharpoons RSSH + RSH \quad (2)$$

$$RSSH + H_2S \rightleftharpoons RSH + HSSH \quad (3)$$

$$nHSSH \rightleftharpoons HS_{(n+1)}H + (n-1)H_2S \quad (n = 1 - 8) \quad (4)$$

and/or

$$RSSH + HS_nH \rightleftharpoons RSH + HS_{(n+1)}H \quad (5)$$

Even at a slight excess of sulfide, all the DTNB is consumed to produce 2 mol equivalents of TNB (Table 1A), indicating that the equilibrium constants of reactions 2 - 5 are large. Hence, the equilibria of these reactions are expected to be largely shifted to the right under the conditions of our kinetic experiments (see next section), making them practically irreversible. Therefore, based on this model, the observed different stoichiometric ratios in Table 1 are due to the kinetically driven partitioning of sulfide in reactions 2 - 5 at the applied concentrations.

3.2. Kinetics of the reaction of DTNB with sulfide

To establish the rate law and to get a deeper insight into the mechanism, we undertook a comprehensive kinetic study on the reaction of DTNB with sulfide under different concentration conditions.

3.2.1. Excess of DTNB over sulfide

Initially the kinetic runs were performed under pseudo-first-order conditions using an excess of DTNB over sulfide. Figure 2A shows that at a 100 fold excess of DTNB (i.e. when 1 sulfide liberates 1 TNB; see Table 1B), the observed kinetic traces fit well to a single exponential equation indicating first order dependence of the rate law on sulfide.

Under these conditions both the observed stoichiometry and kinetic data is consistent with the bimolecular reaction of DTNB with sulfide (reaction 2), suggesting that 100 fold excess of DTNB is necessary for reaction 2 to dominate over reaction 3.

We also found that at lower DTNB concentrations, where more than 1 TNB molecule is liberated per sulfide (indicating a multistep process), the kinetic traces retained their exponential character (Figure S1). In addition, the calculated pseudo-first-order rate constants (k_{obs}) at 320 nm and at 412 nm (representing the decay of DTNB and the formation of TNB) agree within the experimental error at all concentrations (for a representative case see Figure S1). The k_{obs} vs DTNB plot was found to be linear with the fitted line passing through the origin, showing that the reaction is first order for DTNB. At first sight these are controversial because the noted change in stoichiometry should also be associated with a marked change in the kinetic pattern. As it will be shown later, the lack of such complication is most likely due to a unique set of kinetic parameters which yields a simple kinetic behavior. It is concluded that the rate determining step in the model is reaction 2 which is followed by a much faster release of the second TNB. In other words, sulfide reacts much faster with RSSH than with RSSR (DTNB). In addition, the non-detectable intercept in Figure 2B suggests that the equilibrium in reaction 2 is practically irreversible. At pH = 7.4, the apparent second-order rate constant of $k_2^{app} = 881 \pm 15$ $M^{-1}s^{-1}$ for reaction 2 can thus be obtained from the slope of the line on Figure 2B.

3.2.2. Excess of sulfide over DTNB

Despite the fact that under these conditions 2 mol equivalents of TNB were generated per DTNB molecule in a multistep process (see Table 1B), the observed kinetic traces fit well to a single exponential equation at all concentrations (Figure 2C). In addition, regardless of the 1:2

stoichiometry, the obtained pseudo-first-order rate constants for the consumption of DTNB or the production of TNB exhibit a linear dependence on the sulfide concentration with an intercept at the origin (Figure 2D). Furthermore, k_2^{app} = 893 ± 19 $M^{-1}s^{-1}$ that was obtained from the linear fit was similar to the one obtained at excess of DTNB over sulfide (where the calculated k_2^{app} was 881 ± 15 $M^{-1}s^{-1}$). These observations are consistent with the proposed kinetic model, where the rate constant for reaction 3 is more than 10 times larger than the rate constant for reaction 2 and the subsequent reaction steps are much faster than reactions 2 and 3 under any of the applied conditions.

It has to be noted that a slow reaction was also observed in our reaction systems albeit with much smaller absorbance changes. This reaction was more prominent at excess sulfide, and its contribution to the total absorbance changes decreased with the increase in the DTNB concentration at excess DTNB and was not observed at a 100 fold excess of DTNB over sulfide (i.e. at 1:1 stoichiometric ratios). We hypothesize that this reaction could represent disproportionation of slower reacting polysulfides (to liberate sulfide and TNB eventually), which only start operating when TNB-persulfide is consumed. Consistent with this the rate of this reaction was independent of the sulfide concentration, but a more detailed investigation of this minor reaction is outside the scope of the present study. The stoichiometric ratios in Table 1 include the absorbance changes of this step.

3.2.3. Kinetic simulations

The kinetic traces were modelled using the proposed mechanism (reactions 2 - 5, see detailed description of the model in SI) and the average of the measured value for k_2 = 889 $M^{-1}s^{-1}$ [1]. The simulated kinetic traces gave similar pseudo-first-order rate constant values as the experimental ones (see Figure 3A for the two extreme scenarios). These results are also consistent with the noted differences in the stoichiometry and the fact that the exponential character is maintained regardless of the contributions of reactions 3 – 5 to the generation of TNB. Furthermore, consistent with the experimental data, the calculated k_{obs} values from the simulated kinetic traces exhibited a linear dependence on the actual reactant concentration that was used in excess with an intercept at the origin and slopes of 874 $M^{-1}s^{-1}$ and 853 $M^{-1}s^{-1}$ at excess of DTNB and sulfide, respectively (Figures 3 B&C). The results are in agreement with the experimentally obtained apparent second-order rate constants from the linear fits on Figures 2B and 2D (881 $M^{-1}s^{-1}$ and 893 $M^{-1}s^{-1}$, respectively). Thus, kinetic modelling corroborates that our simple mechanism adequately describes the experimental data that was collected in a wide concentration range. Furthermore, the simulations also provided an approximate range for the apparent second-order rate constant of reaction 3 at pH = 7.4 of $k_3 = 5 \times 10^3 – 5 \times 10^4$ $M^{-1}s^{-1}$, because if k_3 were outside of this range, than the simulated lines would substantially deviate from the experimental data (see dashed lines on Figures 3 B&C).

3.2.4. pH dependence

In the 6 > pH > 10 pH region the rate of the reaction was found to increase with the pH and plateau at pH > 9 (Figure 4).

The apparent (pH dependent) second-order rate constants (that were calculated by dividing the observed pseudo-first-order rate constants by the concentrations of the corresponding reagent in excess) exhibit similar pH dependencies in the two series of experiments where either sulfide or DTNB was used in excess over the other, suggesting no change in the rate determining step throughout the investigated pH range. The pH dependence at pH < 6 could not be studied because we observed immediate sulfur precipitation making the system unsuitable for stopped-flow analysis. This is consistent with the disproportionation of polysulfides to give sulfur and H_2S, which is an acid catalyzed process according to the following equation:

$$HS_{(n+1)}^- + H^+ \rightarrow n/8S_8 + H_2S \qquad (n = 1 - 8) \qquad (6)$$

Taking into account that

i) the two ionizable functional groups on DTNB are carboxylic acids groups, which only start to deprotonate at very low pH values ($pK_a \sim 1.6$) [34],

ii) the acid dissociation constant of $HS^- \geq 13$ and

iii) based on a large body of literature, thiol-disulfide exchange reactions occur via a nucleophilic attack of the thiolate form on the disulfide moiety [31],

the observed pH profile most likely reflects the acid dissociation of H_2S to give the reacting HS^- species consistent with the following model:

$$H_2S \rightleftharpoons HS^- + H^+ \qquad K_a^{H_2S} = [HS^-][H^+]/[H_2S] = 2.45 \times 10^{-7}\ M^{-1} \text{ at } I = 1\ M \text{ [35]} \quad (7)$$

$$DTNB + HS^- \xrightarrow{k_8} \text{products} \qquad (8)$$

Using the pre-equilibrium assumption for reaction 7 the following rate law can be derived from the model:

$$d[DTNB]/dt = k_8 \cdot K_a^{H_2S}/(K_a^{H_2S} + H^+) \cdot [sulfide]_{tot} \cdot [DTNB] \qquad (9)$$

The solid line in Figure 4 represents the fit of the experimental data points to equation 9, which gave the pH independent rate constant of k_8 = 1045 ± 11 $M^{-1}s^{-1}$ when the pK_a of hydrogen sulfide was set to p$K_a^{H_2S}$ = 6.61 (at I = 1 M [33]). Equally good fits were obtained when $K_a^{H_2S}$ was used as a floating parameter with the fitted values of k_8 = 1090 ± 12 $M^{-1}s^{-1}$ and p$K_a^{H_2S}$ = 6.79.

3.3. Reduction of cystine and GSSG by sulfide

In order to extend the results discussed above to more biologically relevant systems we studied the reactions of sulfide with cystine and GSSG. First, we investigated the product speciation in the reaction of cystine with sulfide by ^{1}H-NMR spectroscopy.

A

B

The first red spectrum characterizes cystine in the absence of sulfide in Figure 5A. Due to the symmetric nature of the molecule the α and β protons in the two cysteine moieties are equivalent. The β protons are represented by the doublet of doublets (due to coupling with each other and with the α proton) at δ = 3.17 ppm and δ = 3.36 ppm and the chemical shift of the α proton is δ = 4.11 ppm under the applied experimental conditions. Upon titration with sulfide, the formation of cysteine (β protons at 3.02 and 3.09 ppm and α proton at δ = 3.96 ppm) is accompanied by the appearance of a new Cys derivative with β protons at 3.15 and 3.37 ppm and α proton at δ = 4.18 ppm. Based on our results in the DTNB system and consistent with earlier reports [24,36] we propose that the new Cys derivative could represent the Cys-persulfide species. Because the peaks are better resolved in the α proton region (Figure 5B), we made an attempt to estimate the

relative concentrations of cystine, cysteine and the new Cys derivative based on the relative integrals of their α protons as a function of added sulfide (Figure 6A).

The model that was established for the DTNB system, would predict a bell shaped behavior for the concentration of the Cys-persulfide with increasing sulfide concentrations. Notwithstanding, Figure 6A shows that the relative concentrations of Cys and Cys-persulfide reached a plateau at a ~ 1 : 3 cystine : sulfide ratio and instead of a consecutive decline, it slowly started to increase further at higher sulfide concentrations. We hypothesize that at higher sulfide concentrations we introduce enough polysulfides (as inevitable contaminants in our sulfide stock solutions) to perturb the equilibria of reactions 2 and 3 in the cystine-sulfide system. This would not be surprising in light of our previous report, where traces amounts of polysulfides in the presence of a large excess of sulfide was enough for efficient persulfide formation on the active site Cys residues of the *Phosphatase and tensin homolog* (PTEN) protein [17]. To corroborate this assumption we have repeated the NMR titration experiment in the presence (Figure 6C) and absence (Figure 6B) of intentionally generated polysulfides in our sulfide reagent solutions. The experiment was conducted at pH 8 to avoid sulfur precipitation. Indeed the relative Cys-persulfide : Cys ratios increased in the presence of preformed polysulfides, which corroborates our hypothesis and the proposed model. It has to be noted that at higher sulfide concentrations another set of peaks appeared in the β proton region at δ = 2.90 and 3.55 ppm, suggesting the formation of an additional Cys derivative. This could potentially be due to an alkyl

hydrotrisulfide (i.e. CyS-S-SH) or a dialkyl-trisulfide (i.e. CyS-S-SCy) species [9,22,37,38]. A structural characterization of the "new" Cys derivatives is outside the scope of the present study, but consistent with the proposed structures we confirmed that all of them are readily reduced in the presence of DTT to give cysteine. These observations show that the chemistry of these systems can be considerably more complex and certainly system specific.

Due this complexity we only investigated the kinetic nature of the reactions of cystine and GSSG under one set of experimental conditions, i.e. at an excess of sulfide over the disulfide species, in order to get an approximate number for the relative half lifes of these reactions under biologically relevant conditions. The kinetic analysis is further complicated by the fact that, unlike to TNB and DTNB, there is not a characteristic band in the Uv-vis region that could be assigned to a single reagent or reaction product in the cystine or glutathione systems. The observed kinetic traces were recorded using stopped-flow spectroscopy at 300 nm, where polysulfide and persulfide species were shown to absorb [36,39]. The observed kinetic traces reflect the above mentioned complications and even at a 25 fold excess of sulfide they exhibit an induction period, which is indicative of multistep processes (Figure 7). Nevertheless, these experiments show that i) the reduction of cystine and GSSG is significantly slower than the reduction of DTNB (consistent with a previous kinetic study on the reduction of cystine with sulfide that was conducted under alkaline conditions [24]) and ii) the intermediate persulfide species are considerably less reactive compared to TNB-SSH (which is in agreement with the NMR data).

4. Discussion

Accumulating evidence suggest that Cys-persulfides are abundant in cellular systems with peculiar biological functions [7,8,9,19]. However, the molecular mechanisms of persulfide formation and degradation in vivo remains largely elusive. A number of models for persulfide formation were proposed including the reactions of sulfide with Cys sulfenic acid [10,20,40,41], the reaction of polysulfides with reduced thiol species [10,17] as well as sulfide-mediated reduction of disulfide bonds [21,22]. The biological feasibility of this latter reaction is however challenged from the kinetic standpoint based on early studies [23] reporting relatively slow rates and also on thermodynamic grounds considering the low reduction potential of sulfide compared to the largely abundant glutathione system in the cytosol [27]. However, Li and Lancaster Jr. recently pointed out that the S^0/HS^- and GSSG/GSH redox potentials -which were used in the latter study to argue against the thermodynamic feasibility of sulfide-mediated disulfide reduction in a cytosol like environment- were not comparable, because they were referenced to different standards [42].

To obtain a deeper insight into the kinetic and thermodynamic properties of the title reaction we studied the sulfide-mediated reduction of DTNB, cystine and GSSG as model disulfides. First we conducted a comprehensive mechanistic study on the reaction of DTNB with sulfide. The experimentally established rate law exhibits first order dependency for both sulfide and DTNB with an apparent second-order rate constant of 889 ± 12 $M^{-1}s^{-1}$ at pH = 7.4. The pH dependence of the apparent second-order rate constants revealed that the reactive sulfide species is the bisulfide anion, consistent with the reaction proceeding through a nucleophilic attack of HS^- on the disulfide moiety with a pH independent second-order rate constant of 1090 ± 12 $M^{-1}s^{-1}$. At an excess of sulfide, two TNB is released per DTNB in a multistep process, where the oxidizing equivalents are quantitatively converted to give inorganic polysulfides. We proposed a

model that is consistent with the experimental data in which the reaction of DTNB with sulfide is followed by the reduction of the intermediate TNB-persulfide species to yield HSSH and TNB. HSSH than either disproportionates or reacts with the remaining TNB-persulfides to eventually result in the appropriate distribution of polysulfides. The kinetic data indicated that the reduction of the intermediate TNB-persulfide species (reaction 3) has a larger second-order rate constant than the reduction of DTNB by sulfide (reaction 2). However, a 100 fold excess of DTNB was enough to quantitatively consume sulfide for the reduction of DTNB without the concomitant reaction steps taking place, allowing us to provide a range for the apparent second-order rate constant of $5 \times 10^3 - 5 \times 10^4$ $M^{-1}s^{-1}$ for reaction 3.

The reduction of cystine and GSSG at pH = 7.4 clearly occur via more complicated mechanisms as indicated by the product distribution and kinetic analysis. The most important observations in these systems are: 1) the rate of the reactions are considerably slower than for DTNB 2) the Cys-persulfide derivatives are significantly more stable than TNB-persulfide 3) the reactions proceed via multistep equilibrium processes, where the addition of polysulfide shifts the equilibria towards more persulfide generation and 4) additional Cys derivatives can be generated in the reaction beside cysteine and Cys-persulfide.

4.1. Potential physiological relevance

The observed ~ 3 orders of magnitude difference in the reduction rates of DTNB and GSSG predicts that in a biological environment a similarly large variability is expected in the reactivity of disulfides with sulfide (just as in the case of Cys thiol-disulfide exchange reactions) [31]. It is expected that activated disulfides, such as Grx, Trx, PDI , Mia 40 or the Dsb family of proteins, will react much faster with sulfide compared to building block disulfide moieties,

which serve to stabilize protein secondary structures. Furthermore, our data predict that the relative thermodynamic stabilities of disulfides and the corresponding persulfide species (which apparently determines their speciation under the applied conditions) also vary on a wide scale. We showed that DTNB is efficiently reduced by sulfide in a practically irreversible manner even at stoichiometric ratios of the reactants. Moreover, thermodynamically favorable formation of inorganic polysulfides via sulfide-mediated rapid reduction of the intermediate TNB-persulfide derivative was observed. These observations suggest that activated disulfides (such as in DTNB) will react favorably and rapidly with sulfide and potentially generate polysulfide species, which are increasingly recognized important mediators in sulfide biology [43,44,45]. On energetic grounds the other extreme is represented by our previous study on the efficient oxidation of PTEN and roGFP by polysulfides [17]. In that work we demonstrated that trace amounts of polysulfides that are inevitably found in sulfide stock solutions are enough to completely oxidize the protein thiols to the corresponding persulfide derivatives. The cystine-sulfide system lies between these two extremes, where the oxidizing equivalents were distributed among Cys-persulfide and inorganic polysulfide species, with potential formation of dialkyl tri(poly)sulfide and hydropolysulfide Cys derivatives [9,25] under certain conditions as predicted by product analyses.

Collectively, our results demonstrate that the reduction of disulfide species by sulfide is largely system specific, predicting tight regulation from both the thermodynamic and kinetics perspective, which in our view signifies biological feasibility. Although, from the thermodynamic standpoint, we agree with the notion that in a reducing cytosolic environment the glutathione system will govern the distribution of reduced and oxidized thiol species [27], we propose that in a more oxidizing environment, like the endoplasmic reticulum, the mitochondria

or the mitochondrial intermembrane space, reactive disulfides could potentially be prominent reaction partners of sulfide. In fact, in the mitochondrial catabolic pathway of sulfide the first proposed reaction step is the reduction of the intramolecular Cys160-Cys356 disulfide bond of *sulfide quinone reductase* (SQR) by sulfide to give a persulfide intermediate species [46,47]. Furthermore, due to the fact that considerable steady-state concentrations were reported for free sulfide as well as persulfide species in cellular systems (including in the cytosol), the above described thermodynamic differences are likely to play a role in the distribution of sulfane sulfur among protein and peptide Cys residues.

In conclusion, the most important take home message of this work is that the reduction of disulfides by sulfide occurs via multistep equilibria along the disulfide ⇌ persulfide ⇌ inorganic polysulfides axis. We propose that the chemical nature of the disulfide moiety (which is orchestrated by the surrounding amino acid functional groups in proteins and peptides) [31] will play a major role in the kinetic feasibility of its reduction by sulfide and the thermodynamic stabilities of the corresponding disulfide vs persulfide vs inorganic polysulfide species will determine the speciation of sulfane sulfur entities in these molecules.

5. Acknowledgements

Financial support from FP7-PEOPLE-2010-RG (Marie Curie International Reintegration Grant; grant No.: PIRG08-GA-2010-277006) and The Hungarian National Science Foundation (OTKA; grant No.: K 109843) for P.N and from the Hungarian Development Plan (grant No.: TAMOP-4.2.2/B-10/1-2010-0024) and The Hungarian National Science Foundation (OTKA; grant No.: NK 105156) for I.F are greatly acknowledged. V.A. is a PhD scholar funded by the FP7-PEOPLE-2010-RG (Marie Curie International Reintegration Grant; grant No.: PIRG08-GA-2010-277006) grant.

6. List of abbreviations

DNTB: 5,5'-dithiobis-(2-nitrobenzoic acid) - Ellman's reagent
TNB: 5-thio-2-nitrobenzoic acid
Cys: cysteine
GSSG: oxidized glutathione
DSS: 4,4-dimethyl-4-silapentane-1-sulfonic acid
PTEN: phosphatase and tensin homologe
DTT: dithiothreitol
Grx: glutaredoxin
Trx: thioredoxin
PDI: protein disulfide-isomerase
Mia 40: Mitochondrial intermembrane space import and assembly protein 40Dsb family: disulfide bond protein family
roGFP: redox sensitive green fluorescent protein

7. Footnotes

[1] Sulfide will be used here after as a generic term to include all the different protonation isomers of hydrogen sulfide. Distinction between the different protonated forms is made only when it is required by the clarity of discussion.

8. References

[1] K. Abe, H. Kimura, The possible role of hydrogen sulfide as an endogenous neuromodulator, J Neurosci 16 (1996) 1066-1071.

[2] R.O. Beauchamp, J.S. Bus, J.A. Popp, C.J. Boreiko, D.A. Andjelkovich, A Critical-Review of the Literature on Hydrogen-Sulfide Toxicity, Crc Cr Rev Toxicol 13 (1984) 25-97.

[3] H. Kimura, The physiological role of hydrogen sulfide and beyond, Nitric Oxide-Biol Ch 41 (2014) 4-10.

[4] R. Wang, Physiological Implications of Hydrogen Sulfide: A Whiff Exploration That Blossomed, Physiol Rev 92 (2012) 791-896.

[5] C. Szabo, Hydrogen sulphide and its therapeutic potential, Nat Rev Drug Discov 6 (2007) 917-935.

[6] H. Kimura, H2S2014 in Kyoto: The 3rd International Conference on H2S in Biology and Medicine, Nitric Oxide (2014). This issue, *epub ahead of print.*

[7] A.K. Mustafa, M.M. Gadalla, N. Sen, S. Kim, W.T. Mu, S.K. Gazi, R.K. Barrow, G.D. Yang, R. Wang, S.H. Snyder, H2S Signals Through Protein S-Sulfhydration, Sci Signal 2 (2009) ra72.

[8] B.D. Paul, S.H. Snyder, H2S signalling through protein sulfhydration and beyond, Nat Rev Mol Cell Bio 13 (2012) 499-507.

[9] K. Ono, T. Akaike, T. Sawa, Y. Kumagai, J.M. Fukuto, J. Lin, M. Xian, P. Nagy, A.J. Hobbs, D.A. Wink, D.J. Tantillo, The Redox Chemistry and Chemical Biology of H2S, Hydropersulfides and Derived Species: Implications to Their Possible Biological Activity and Utility, Free Radical Bio Med 77 (2014) 82-94.

[10] P. Nagy, Z. Palinkas, A. Nagy, B. Budai, I. Toth, A. Vasas, Chemical aspects of hydrogen sulfide measurements in physiological samples, Biochim. Biophys. Acta-Gen. Subj. 1840 (2014) 876-891.

[11] S.L. Melideo, M.R. Jackson, M.S. Jorns, Biosynthesis of a Central Intermediate in Hydrogen Sulfide Metabolism by a Novel Human Sulfurtransferase and Its Yeast Ortholog, Biochemistry-Us 53 (2014) 4739-4753.

[12] N. Sen, Bindu D. Paul, Moataz M. Gadalla, Asif K. Mustafa, T. Sen, R. Xu, S. Kim, Solomon H. Snyder, Hydrogen Sulfide-Linked Sulfhydration of NF-κB Mediates Its Antiapoptotic Actions, Molecular Cell 45 (2012) 13-24.

[13] K.X. Zhao, Y.J. Ju, S.S. Li, Z. Altaany, R. Wang, G.D. Yang, S-sulfhydration of MEK1 leads to PARP-1 activation and DNA damage repair, Embo Rep 15 (2014) 792-800.

[14] A.K. Mustafa, G. Sikka, S.K. Gazi, J. Steppan, S.M. Jung, A.K. Bhunia, V.M. Barodka, F.K. Gazi, R.K. Barrow, R. Wang, L.M. Amzel, D.E. Berkowitz, S.H. Snyder, Hydrogen Sulfide as Endothelium-Derived Hyperpolarizing Factor Sulfhydrates Potassium Channels, Circ Res 109 (2011) 1259-U1169.

[15] J.M. Hourihan, J.G. Kenna, J.D. Hayes, The Gasotransmitter Hydrogen Sulfide Induces Nrf2-Target Genes by Inactivating the Keap1 Ubiquitin Ligase Substrate Adaptor Through Formation of a Disulfide Bond Between Cys-226 and Cys-613, Antioxid Redox Sign 19 (2013) 465-481.

[16] N. Krishnan, C.X. Fu, D.J. Pappin, N.K. Tonks, H2S-Induced Sulfhydration of the Phosphatase PTP1B and Its Role in the Endoplasmic Reticulum Stress Response, Sci Signal 4 (2011) ra86.
[17] R. Greiner, Z. Palinkas, K. Basell, D. Becher, H. Antelmann, P. Nagy, T.P. Dick, Polysulfides Link H2S to Protein Thiol Oxidation, Antioxid Redox Sign 19 (2013) 1749-1765.
[18] G.D. Yang, K.X. Zhao, Y.J. Ju, S. Mani, Q.H. Cao, S. Puukila, N. Khaper, L.Y. Wu, R. Wang, Hydrogen Sulfide Protects Against Cellular Senescence via S-Sulfhydration of Keap1 and Activation of Nrf2, Antioxid Redox Sign 18 (2013) 1906-1919.
[19] T. Ida, T. Sawa, H. Ihara, Y. Tsuchiya, Y. Watanabe, Y. Kumagai, M. Suematsu, H. Motohashi, S. Fujii, T. Matsunaga, M. Yamamoto, K. Ono, N.O. Devarie-Baez, M. Xian, J.M. Fukuto, T. Akaike, Reactive cysteine persulfides and S-polythiolation regulate oxidative stress and redox signaling, P Natl Acad Sci USA 111 (2014) 7606-7611.
[20] P. Nagy, C.C. Winterbourn, Reaction of Hydrogen Sulfide with the Neutrophil Oxidant Hypochlorous Acid to Generate Polysulfides, Chem Res Toxicol 23 (2010) 1541-1543.
[21] N.E. Francoleon, S.J. Carrington, J.M. Fukuto, The reaction of H2S with oxidized thiols: Generation of persulfides and implications to H2S biology, Arch Biochem Biophys 516 (2011) 146-153.
[22] R.W. Nielsen, C. Tachibana, N.E. Hansen, J.R. Winther, Trisulfides in Proteins, Antioxid Redox Sign 15 (2011) 67-75.
[23] D. Cavallini, G. Federici, E. Barboni, Interaction of Proteins with Sulfide, European Journal of Biochemistry 14 (1970) 169-174.
[24] D.K. Liu, S.G. Chang, Kinetic-Study of the Reaction between Cystine and Sulfide in Alkaline-Solutions, Can J Chem 65 (1987) 770-774.
[25] J.I. Toohey, Sulfur signaling: Is the agent sulfide or sulfane?, Anal Biochem 413 (2011) 1-7.
[26] J.I. Toohey, The conversion of H2S to sulfane sulfur, Nat Rev Mol Cell Bio 13 (2012) 804-804.
[27] O. Kabil, R. Banerjee, Redox Biochemistry of Hydrogen Sulfide, J Biol Chem 285 (2010) 21903-21907.
[28] D.H. Zhang, I. Macinkovic, N.O. Devarie-Baez, J. Pan, C.M. Park, K.S. Carroll, M.R. Filipovic, M. Xian, Detection of Protein S-Sulfhydration by a Tag-Switch Technique, Angew Chem Int Edit 53 (2014) 575-581.
[29] C.E. Paulsen, K.S. Carroll, Cysteine-Mediated Redox Signaling: Chemistry, Biology, and Tools for Discovery, Chem Rev 113 (2013) 4633-4679.
[30] G.L. Ellman, A colorimetric method for determining low concentrations of mercaptans, Arch Biochem Biophys 74 (1958) 443-450.
[31] P. Nagy, Kinetics and Mechanisms of Thiol-Disulfide Exchange Covering Direct Substitution and Thiol Oxidation-Mediated Pathways, Antioxid Redox Sign 18 (2013) 1623-1641.
[32] P. Eyer, F. Worek, D. Kiderlen, G. Sinko, A. Stuglin, V. Simeon-Rudolf, E. Reiner, Molar absorption coefficients for the reduced Ellman reagent: reassessment, Anal Biochem 312 (2003) 224-227.
[33] A.S. Nashef, D.T. Osuga, R.E. Feeney, Determination of Hydrogen-Sulfide with 5,5'-Dithiobis-(2-Nitrobenzoic Acid), N-Ethylmaleimide, and Parachloromercuribenzoate, Anal Biochem 79 (1977) 394-405.

[34] P. Nagy, G.N.L. Jameson, C.C. Winterbourn, Kinetics and Mechanisms of the Reaction of Hypothiocyanous Acid with 5-Thio-2-nitrobenzoic Acid and Reduced Glutathione, Chem Res Toxicol 22 (2009) 1833-1840.
[35] R.M. Smith, A.E. Martell, Critical Stability Constants, Plenun Press, New York, 1976.
[36] G.S. Rao, G. Gorin, Reaction of Cystine with Sodium Sulfide in Sodium Hydroxide Solution, The Journal of Organic Chemistry 24 (1959) 749-753.
[37] M. Moutiez, M. Aumercier, E. Teissier, B. Parmentier, A. Tartar, C. Sergheraert, Reduction of a Trisulfide Derivative of Glutathione by Glutathione Reductase, Biochem Bioph Res Co 202 (1994) 1380-1386.
[38] B. Parmentier, M. Moutiez, A. Tartar, C. Sergheraert, Preparation of Trisulfide Derivatives of Cystine and Their Formation as by-Products during Peptide-Synthesis, Tetrahedron Lett 35 (1994) 3531-3534.
[39] W. Giggenbach, Optical-spectra and equilibrium distribution of polysulfide ions in aqueous-solution at 20 degrees., Inorg Chem (1972) 1201–1207.
[40] K.S. Carroll, M.L. Conte, The Chemistry of Thiol Oxidation and Detection, Oxidative stress and redox regulation. Jakob, U. Ed.; Springer: New York 2012, Chapter 1.
[41] O. Kabil, N. Motl, R. Banerjee, H2S and its role in redox signaling, Bba-Proteins Proteom 1844 (2014) 1355-1366.
[42] Q. Li, J.R. Lancaster, Chemical foundations of hydrogen sulfide biology, Nitric Oxide-Biol Ch 35 (2013) 21-34.
[43] Y. Kimura, Y. Mikami, K. Osumi, M. Tsugane, J. Oka, H. Kimura, Polysulfides are possible H2S-derived signaling molecules in rat brain, Faseb J 27 (2013) 2451-2457.
[44] S. Koike, Y. Ogasawara, N. Shibuya, H. Kimura, K. Ishii, Polysulfide exerts a protective effect against cytotoxicity caused by t-buthylhydroperoxide through Nrf2 signaling in neuroblastoma cells, Febs Lett 587 (2013) 3548-3555.
[45] H. Kimura, N. Shibuya, Y. Kimura, Hydrogen Sulfide Is a Signaling Molecule and a Cytoprotectant, Antioxid Redox Sign 17 (2012) 45-57.
[46] M.M. Cherney, Y.F. Zhang, M. Solomonson, J.H. Weiner, M.N.G. James, Crystal Structure of Sulfide:Quinone Oxidoreductase from Acidithiobacillus ferrooxidans: Insights into Sulfidotrophic Respiration and Detoxification, J Mol Biol 398 (2010) 292-305.
[47] O. Kabil, R. Banerjee, Enzymology of H2S Biogenesis, Decay and Signaling, Antioxid Redox Sign 20 (2014) 770-782.

Figure 1. Spectral titration of sulfide with DTNB. Mixing 50 µM sulfide with (5.0, 10.0, 15.0, 20.0, 25.0 µM) DTNB in 100 mM phosphate buffer at pH 7.40, 25 °C and I = 1 M results in a concentration dependent increase of TNB's characteristic absorbance band at 412 nm.

Figure 2. Concentration dependence of the pseudo-first-order rate constant for the reaction of sulfide with DTNB. Representative stopped-flow kinetic trace for the reaction of (A) 500 µM DTNB with 5 µM HS^- or (B) 100 µM sulfide with 1 µM DTNB in 100 mM phosphate buffer at pH 7.40, 25 °C and I = 1 M. Experimental kinetic traces were recorded at 412 nm ((A) blue dots, (B) red rhombs), where the solid black lines represent the corresponding single exponential fits. The pseudo-first-order rate constants exhibit linear dependences on the (C) DTNB and (D)

sulfide concentrations at an excess of DTNB and sulfide, respectively. Linear fits are represented by solid lines with the obtained equations of C) y = 0.881 x - 0.0008 and D) y = 0.893 x - 0.0088.

Figure 3. Kinetic simulations of the reaction of sulfide with DTNB. Simulations were carried out using the proposed model (see reactions 2 - 5 and Supporting Information). A) Representative simulated kinetic traces for the reaction of 500 µM DTNB with 5 µM sulfide (blue triangles) or 500 µM sulfide with 5 µM DTNB (red squares) with solid black lines representing the corresponding single exponential fits of the calculated data. The experimental and simulated pseudo-first-order rate constants agree within the experimental error. At excess DTNB: measured k_{obs} = 0.43 ± 0.01 s^{-1} and calculated k_{obs} = 0.45 s^{-1}; at excess sulfide measured k_{obs} = 0.46 ± 0.02 s^{-1} and calculated k_{obs} = 0.44 s^{-1}. DTNB (B) and sulfide (C) concentration dependences of the pseudo-first-order rate constant for the reaction of sulfide with DTNB. Blue dots and red rhombs are identical to the experimental values presented in Figure 2B and D. Solid black lines show the dependence of the simulated pseudo-first-order rate constant on the concentration of the actual reagent in excess, where in the model the rate constant of reaction (3) was set to be 10 times larger than that of reaction (2) (i.e. r = 10 in Model 1 where r = k_3/k_2; see reactions 2 - 5 and Supporting Information). The equations of the simulated solid lines are (B) y = 0.874 x + 0.0038 and (C) y = 0.853 x - 0.0016. The dashed lines were calculated with r = 100 in panel (B) and r = 3 in panel (C), giving the corresponding equations of (B) y = 0.940 x + 0.0235 and (C) y = 0.740 x - 0.0016, which exhibit considerable deviation from the observed data.

Figure 4. pH dependence of the apparent, reactant concentration independent, second-order rate constant. Data were collected at excess DTNB (blue dots) or sulfide (red rhombs) in 100 mM phosphate buffer at 25 °C, I = 1 M. The kinetic traces were recorded at λ = 412 nm and the solid line represents the corresponding fit of the experimental data to equation 9 using $K_a^{H_2S}$ as a fixed (dashed line) or as a floating (solid line) parameter (see main text for details and for fitted and fixed values).

Figure 5. ^{1}H-NMR titration of L-cystine with sulfide. 3 mM cystine was equilibrated with the indicated amounts of sulfide at pD = 7.40 in 225 mM deuterated phosphate buffer at 25 °C.

Figure 6. Speciation of cystine derivatives as a function of sulfide concentration. Relative distribution of cystine (blue rhombs), cysteine (green triangles) and Cys-persulfide (red dots) - after the reactions of 3 mM cystine with the indicated amounts of sulfide in 225 mM deuterated phosphate buffer reached equilibrium at pD = 7.40 (A) or 8.0 (B&C)- were determined based on the relative integrals of their alpha protons (see Figure 5B). On Figure 6C sulfide reactant solutions contained 50% (relative to $[sulfide]_{tot}$) of sulfane sulfure in the form of inorganic polysulfides (see Methods for experimental details). Error bars represent standard deviations of 3 independent experiments.

Figure 7. Representative kinetic traces (A, C) and half lives (B, D) in the cystine/GSSG-sulfide systems. 1.5 mM of cystine (A, B) or GSSG (C, D) were reacted with 15, 20, 25, 30, 35 mM of sulfide at pH = 7.4 in 100 mM phosphate buffer at 25 ^{o}C and I = 1 M. Kinetic traces were recorded at 300 nm.

Table 1. Stoichiometry of the DTNB - sulfide reaction at various reactant concentrations using either sulfide (A) or DTNB (B) in excess at pH = 7.4 in 100 mM phosphate buffer at 25°C and I = 1 M (NaCl).